A modular paper-and-plastic device for tuberculosis nucleic acid amplification testing in limited-resource settings

Navjot Kaur[a], Joy S. Michael[b], Bhushan J. Toley[a]*

[a] Department of Chemical Engineering
Indian Institute of Science
Bangalore, India
560012

[b] Department of Microbiology
Christian Medical College
Vellore, India
632004

*Correspondence to:
Bhushan J. Toley
Department of Chemical Engineering
Indian Institute of Science
Bangalore, India, 560012
Phone: +91-80-22933114
Email: bhushan@iisc.ac.in

Supplementary Information

Supplementary Table S1. Sequence of the primers used for loop-mediated isothermal amplification (LAMP) targeting the hspX gene of Mycobacterium tuberculosis

Primer	Sequence	Length
hspXF3	TCATTCGCCGGACTCCG	17
hspXB3	GGAACCGTACGCGAATTCC	19
hspXFIP	ACCTCGTAGCGCCCCTCTTACCTTCGACACCCGGTTGA	38
hspXBIP	GGACGTCGACATTATGGTCCGCGTCGAAGTCCTTCTGCTCG	41
hspXFLP	CATCTCGTCTTCCAGCCGCA	20
hspXBLP	GATGGTCAGCTGACCATCAAGGC	23

Supplementary Table S2. Intensity analysis for TB testing from clinical samples in FLIPP-NAAT

FLIPP-NAAT devices in Figure S7							
Panel A		**Panel B**		**Panel C**		**Panel D**	
Sample	Mean Intensity	Sample	Mean Intensity	Sample	Mean Intensity	Sample	Mean Intensity
1_I	131.694	4_I	148.338	7_I	131.717	10_I	140.269
1_II	131.155	4_II	132.139	7_II	138.828	10_II	148.547
1_N	59.919	4_N	75.363	7_N	96.425	10_N	88.165
1_P	103.337	4_P	133.205	7_P	136.012	10_P	144.787
2_I	78.599	5_I	80.15	8_I	135.932	11_1	146.598
2_II	72.357	5_II	93.591	8_II	139.167	11_2	140.289
2_N	72.792	5_N	86.866	8_N	139.48	11_N	81.309
2_P	129.084	5_P	144.155	8_P	136.698	11_P	121.68
3_I	130.02	6_I	74.723	9_I	125.111	12_I	136.363
3_II	142.195	6_II	83.169	9_II	137.017	12_II	125.492
3_N	53.529	6_N	80.517	9_N	95.614	12_N	87.555
3_P	132.077	6_P	143.867	9_P	144.731	12_P	124.047
Average N, μ	62.080		80.915		**FAILED TEST**		85.676
Stdev N, σ	9.812		5.762				3.794
μ + 3σ	**91.515**		**98.201**				**97.060**

Panel E		Panel F		Panel G		Panel H	
Sample	Mean Intensity	Sample	Mean Intensity	Sample	Mean Intensity	Sample	Mean Intensity
13_I	148.164	16_I	137.858	19_I	107.401	7_I	138.551
13_II	152.811	16_II	153.844	19_II	103.921	7_II	136.752
13_N	74.106	16_N	79.293	19_N	72.018	7_N	62.42
13_P	128.795	16_P	145.859	19_P	144.443	7_P	130.96
14_I	144.289	17_I	98.983	20_I	141.318	9_I	77.025
14_II	136.75	17_II	127.779	20_II	140.77	9_II	72.347
14_N	73.539	17_N	94.537	20_N	75.266	9_N	68.308
14_P	142.134	17_P	135.309	20_P	155.756	9_P	140.805
15_I	97.84	18_I	125.964	8_I	154.339	17_I	62.362
15_II	79.662	18_II	122.638	8_II	151.342	17_II	104.034
15_N	59.614	18_N	68.203	8_N	77.026	17_N	70.985
15_P	136.897	18_P	122.987	8_P	136.573	17_P	119.705
Average N, μ	69.086		80.678		74.770		67.238
Stdev N, σ	8.208		13.221		2.541		4.382
μ + 3σ	**93.711**		**120.342**		**82.392**		**80.383**

Panel I		Panel J		Panel K		Panel L	
Sample	Mean Intensity	Sample	Mean Intensity	Sample	Mean Intensity	Sample	Mean Intensity
21_I	93.876	24_I	77.219	27_I	90.755	30_I	**116.512**
21_II	85.786	24_II	75.518	27_II	133.282	30_II	**117.412**
21_N	90.362	24_N	96.528	27_N	89.745	30_N	**84.555**
21_P	165.242	24_P	141.188	27_P	163.996	30_P	**172.742**
22_I	93.154	25_I	85.603	28_I	151.157	23_I	**166.102**
22_II	137.185	25_II	102.303	28_II	135.874	23_II	**164.343**
22_N	81.847	25_N	95.482	28_N	78.497	23_N	**85.645**
22_P	175.221	25_P	154.224	28_P	186.651	23_P	**163.813**
23_I	100.309	26_I	95.077	29_I	87.29	27_I	**137.726**
23_II	108.33	26_II	78.459	29_II	78.448	27_II	**126.759**
23_N	84.875	26_N	83.922	29_N	70.855	27_N	**63.396**
23_P	140.001	26_P	154.87	29_P	141.929	27_P	**124.234**
Average N, μ	85.683		91.977		79.699		**77.865**
Stdev N, σ	4.297		6.996		9.502		**12.543**
μ + 3σ	98.573		112.964		108.206		**115.493**

FLIPP-NAAT devices in Figure S8							
Panel A		**Panel B**		**Panel C**		**Panel D**	
Sample	Mean Intensity	Sample	Mean Intensity	Sample	Mean Intensity	Sample	Mean Intensity
21_I	135.925	22_I	130.042	23_I	132.657	24_I	**77.424**
21_II	147.213	22_II	120.756	23_II	101.311	24_II	**68.613**
21_N	89.659	22_N	86.674	23_N	86.364	24_N	**77.414**
21_P	133.738	22_P	128.716	23_P	147.642	24_P	**162.502**
21_III	146.462	22_III	160.487	23_III	117.306	24_III	**101.973**
21_IV	99.231	22_IV	103.990	23_IV	114.856	24_IV	**82.618**
21_N	89.728	22_N	92.934	23_N	84.712	24_N	**78.381**
21_P	153.242	22_P	154.586	23_P	163.857	24_P	**182.721**
21_V	135.248	22_V	101.872	23_V	133.351	24_V	**78.424**
21_VI	75.450	22_VI	125.855	23_VI	92.415	24_VI	**77.593**
21_N	99.034	22_N	75.571	23_N	95.106	24_N	**63.299**
23_P	127.270	22_P	124.525	23_P	156.42	24_P	**146.148**
Average N, μ	92.807		85.060				**73.031**
Stdev N, σ	5.393		8.793				**8.442**
μ + 3σ	108.986		111.440				**98.358**
Panel E							
Sample	Mean Intensity	Sample	Mean Intensity	Sample	Mean Intensity	Sample	Mean Intensity
25_I	153.558	25_II	96.774	25_III	127.915	25_IV	**101.607**
25_V	104.304	25_VI	69.424	25_N	79.628	25_P	**192.299**
25_N	98.735	25_P	143.420	25_N	78.534	25_P	**145.520**
Average N, μ	85.632						
Stdev N, σ	11.360						
μ + 3σ	119.714						

Supplementary Table S3. Cost of materials used for fabricating one device

Material	**Size (cm)**	**Area, (cm^2)**	**Cost ($)**	**Cost/ cm2 ($)**	**Area per device (cm^2)**	**Cost ($)**
PSA sheet, A4	21x9.7	623.7	3.34	0.0053	38.92	0.624
Transparency sheet, A4	21x29.7	623.7	0.04	0.00007	20.17	0.001

2.8mm transparent acrylic sheet, A3	29.7x42	1247.4	5.61	0.0045	20.02	0.090
2mm black acrylic sheet, A3	29.7x42	1247.4	5.61	0.0045	18.75	0.084
Standard 17 sheet, A4	21x29.7	623.7	14.25	0.0228	3.741	0.085
Total material cost for one device ($)						**0.885**

Supplementary Table S4. Cost of reagents required for 1000 reactions

Reaction component	**Price ($)**	**Stock conc and volume**	**Used per 12.5ul reaction**	**Cost/1000 reactions, ($)**
FIP	25.652	150,100µM	1.6µM, 0.25µl	0.684
BIP	25.652	150,100µM	1.6µM, 0.25µl	0.684
F3	18.526	350,100µM	0.2µM, 0.25µl	0.026
B3	18.526	350,100µM	0.2µM, 0.25µl	0.026
LF	18.526	350,100µM	1.2µM, 0.375µl	0.318
LB	18.526	350,100µM	1.2µM, 0.375µl	0.318
dNTPs	83.59	10mM, 500µl	1.25µl	208.992
DEPC Water	8.693	100ml	2.25µl	0.196
Pol, Buffer, MgSO4	103.235	8000U/ml, 1600 units	-	
Pol (70% cost)	72.264	8000U/ml, 1600 units	4unit	180.66
Buffer (20%cost)	20.647	10X, 1500µl	1X, 1.25µl	1.721
MgSO4 (10% cost)	10.324	100mM, 1500µl	6mM, 1µl	0.413
Betaine	32.736	5M, 1500µl	0.9M,2.25µl	8.838
SYBR green I	539.290	10000X, 500µl	50X,5µl	26.965
Total cost for **1000** reactions				429.843

Supplementary Figure S1. LAMP reactions in presence of different concentrations of human gDNA

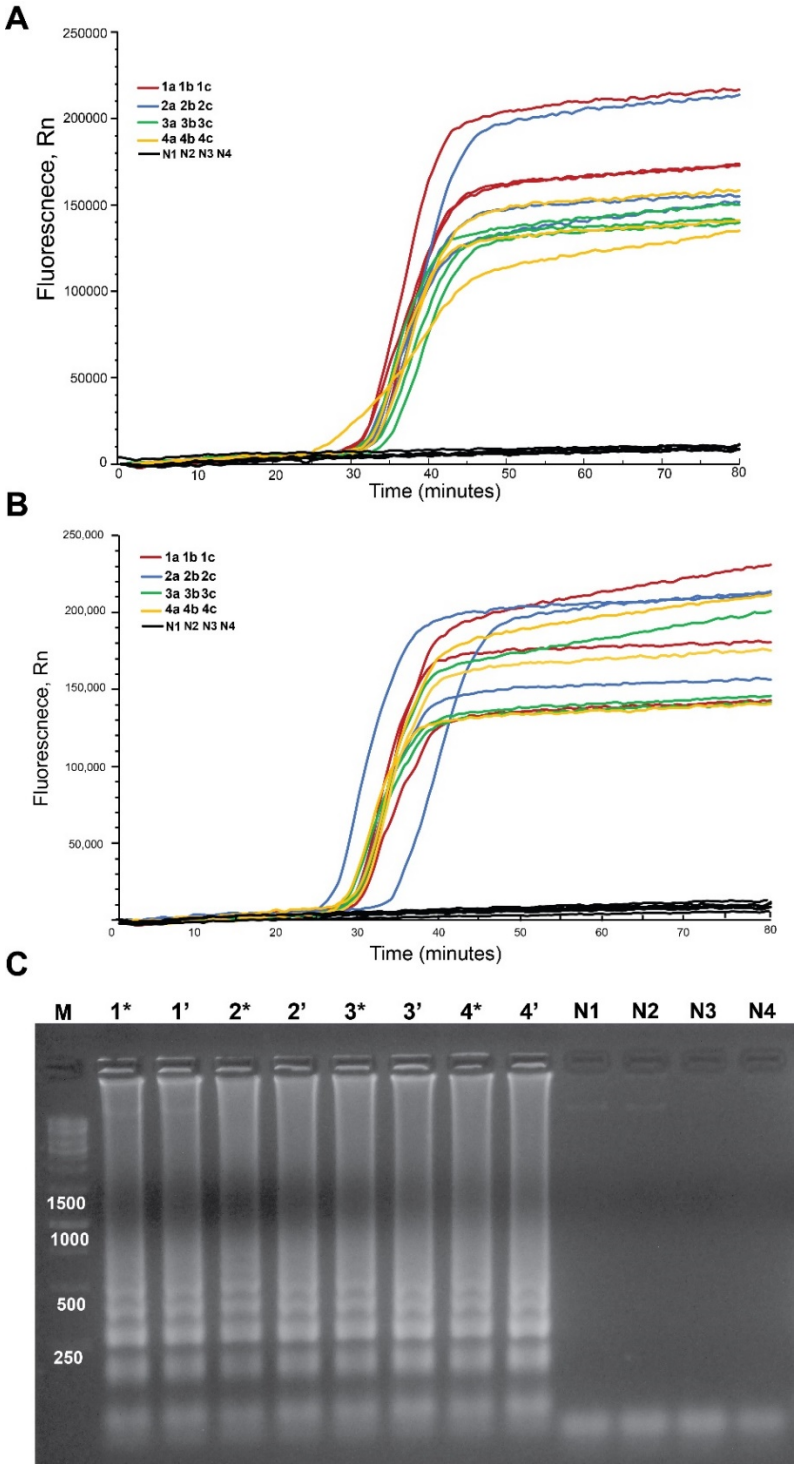

Supplementary Figure S1. LAMP reactions in presence of different concentrations of human gDNA for a reaction time of 80 minutes. Real-time amplification curves for LAMP reactions run with (A) 100 starting copies of Mtb gDNA and (B) 1000 starting copies of Mtb gDNA in presence of different

concentrations of human gDNA. (C) Gel electrophoresis analysis of the LAMP amplicons. 1- $3.1*10^4$, 2- $3.1*10^3$, 3- $3.1*10^2$, 4- $3.1*10$ copies of human gDNA respectively. a, b and c represent triplicates. N- No template control was run in the presence of different concentrations of human gDNA as indicated by 1,2,3 and 4 but no Mtb gDNA was added. * - 100 starting Mtb gDNA copies and '– 1000 starting Mtb gDNA copies. All samples were run in triplicates. All the lanes are from the same gel and the original gel image has been used.

Supplementary Figure S2. Optimization of the reaction temperature

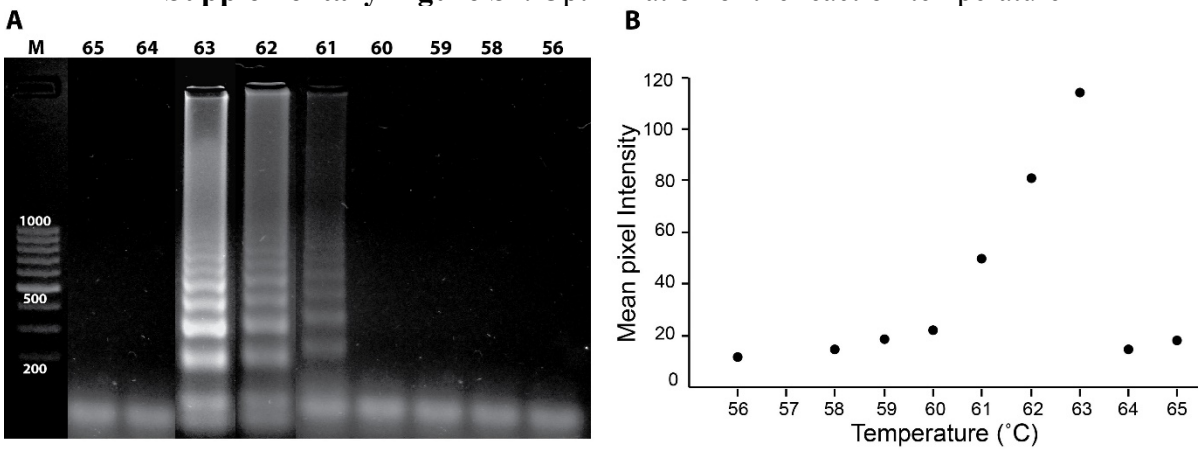

Supplementary Figure S2. Temperature optimization for the LAMP reaction. (A) Gel electrophoresis analysis of LAMP amplicons. Numbers on top of each well indicate the operating reaction temperature in ˚C. The reaction time was 40 minutes. (B) The average pixel intensity for each lane, calculated using ImageJ. Maximum amplification was observed at 63˚C.

A rectangular selection area covering each lane from the well till the bottom was drawn in ImageJ and the mean intensities were calculated. The mean pixel intensity, which is proportional to the total amount of DNA produced was plotted against the respective reaction temperature. Maximum amplification was observed at 63˚C, which was hence chosen as the reaction temperature.

Supplementary Figure S3. Fluorescence imaging using optical filter

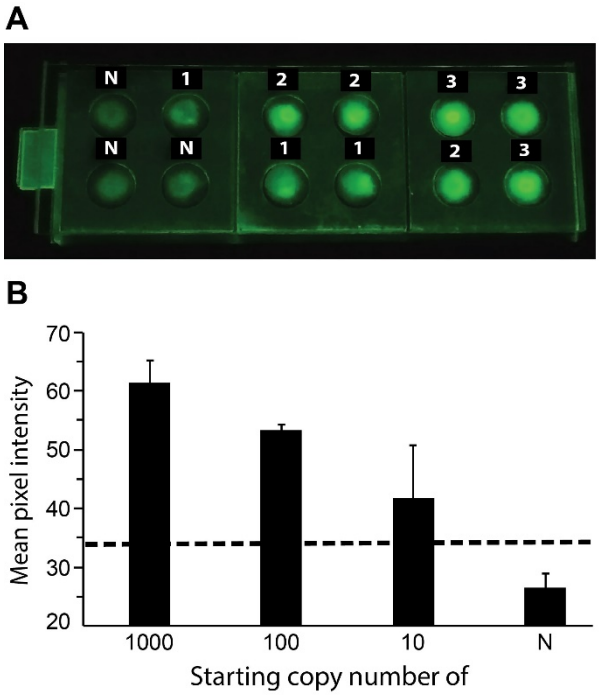

Supplementary Figure S3. Fluorescence imaging using optical filter. (A) End-point fluorescence detection. FLIPP-NAAT was imaged using a 510-550 nm band pass filter. (B) Mean green color intensities for different starting copy numbers of Mtb gDNA. The dashed line represents the threshold value of ($\mu_N+3\sigma_N$).

Fluorescence imaging was also performed using optical filters to check if filters helped in improving the imaging sensitivity. The mean intensities for each of the copy numbers was less than half of the intensities observed for imaging without the filters. While imaging without filters, it was seen that the mean intensities were co-related with the starting copy numbers with statistically significant differences. But for imaging through optical filters, the mean intensities for 100 and 10 copies were not statistically different. Though mean intensities for reactions with 1000 starting copies continued to be statistically higher than 100 copies and same was true for 10 starting copies in comparison with the negative control. Apart from non-specific interaction with single-

stranded DNA, the dye also seemed to have a component of green color even in its unbound state, which led to a prominent green signal in the negative controls when imaged through the filter.

Supplementary Figure S4. Optimization of the concentration of trehalose required for dry-storage of LAMP reagents

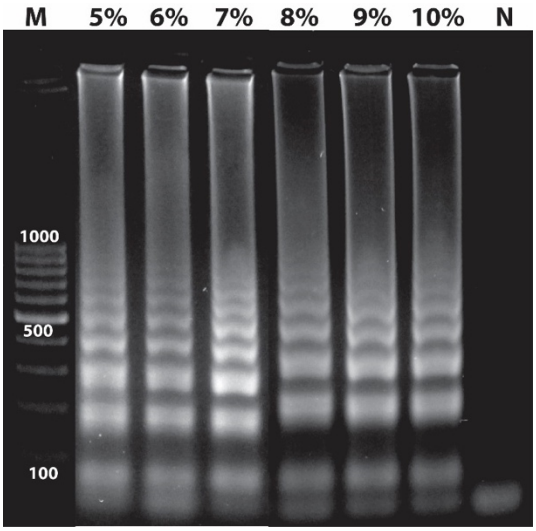

Supplementary Figure S4. Optimization of dry-storage of LAMP reagents. LAMP in tube was conducted with different concentrations of trehalose to check for the effect of trehalose on DNA amplification. LAMP amplicons were analysed using gel electrophoresis. The numbers on top of the wells indicate the percentage of trehalose used. M – DNA ladder, N – no template control.

Supplementary Figure S5. TB testing in FLIPP-NAAT using DNA extracted by conventional techniques

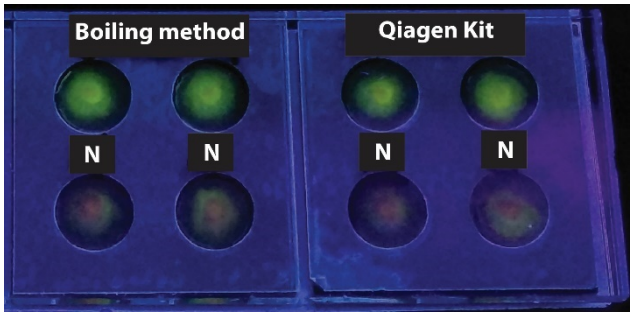

Supplementary Figure S5. LAMP from Mtb gDNA obtained by different DNA extraction methods. Mtb gDNA was extracted from the H37Ra cells using an in-house boiling method and Qiagen DNA extraction kit. The extracted DNA was used for DNA amplification in FLIPP-NAAT. Labels on the top of the reaction zones indicate the technique used for DNA extraction. N- no template control.

Supplementary Figure S6. TB testing for clinical samples in FLIPP-NAAT

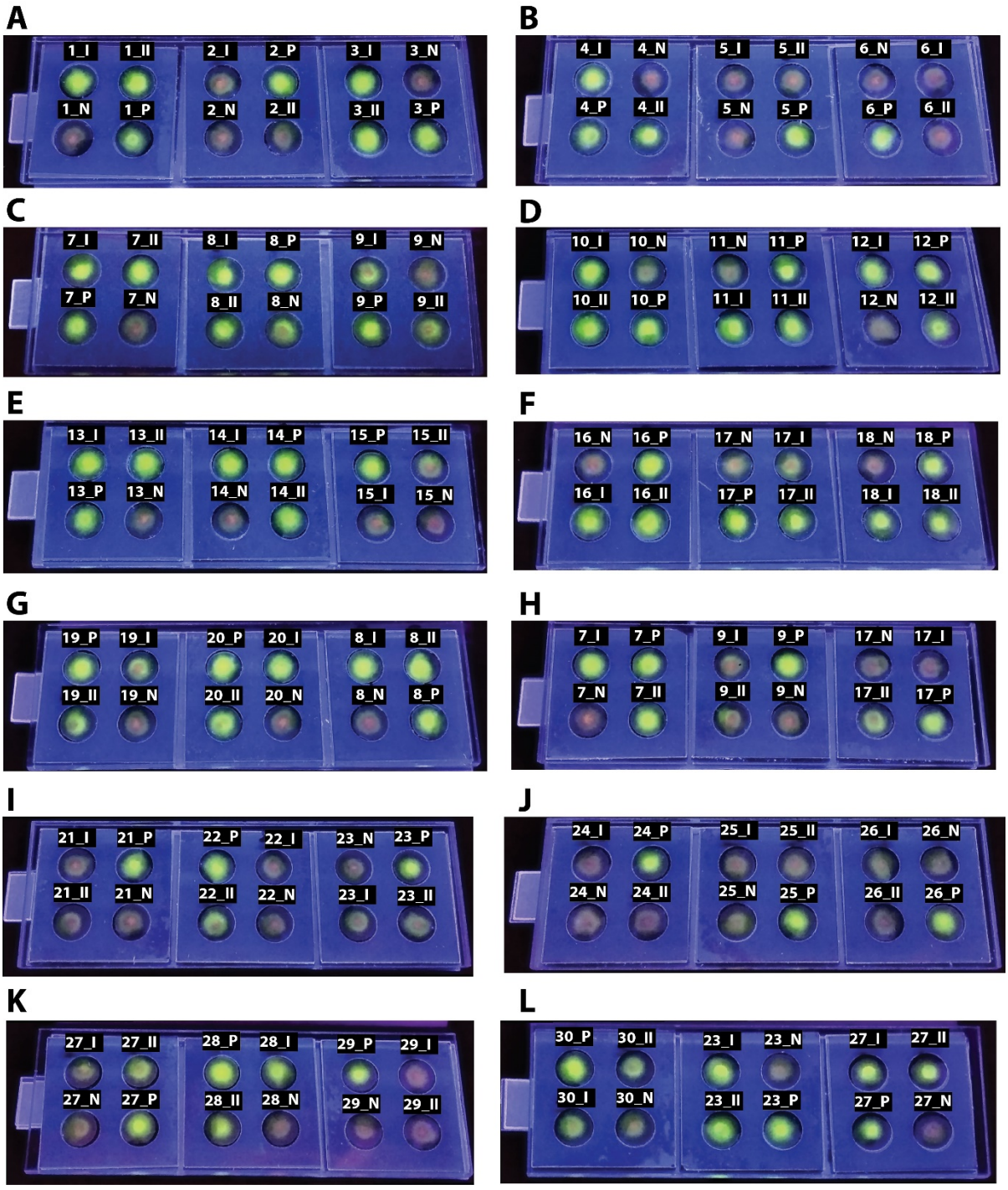

Supplementary Figure S6. TB testing in FLIPP-NAAT for clinical samples. 30 blind clinical samples were tested in FLIPP-NAAT and the results were captured using a cell phone camera. Numbers on top of each testing zone represent the sample number. Each sample was tested in duplicates and suffix 'I' and 'II' represent the duplicates for each sample. N – Negative control. P – Positive control.

The protocol for testing the twenty clinical samples in FLIPP-NAAT is described in the methods section of the main manuscript. Images were captured using a cell phone camera and intensity analysis was done in the green channel using ImageJ. Supplementary Figure S7 shows the end-point images for all the 12 devices used to test the 30 samples. Since one of the negative controls for the device in panel (C) (8_N) showed amplification, this device was declared as a failed test and samples 7, 8 and 9 were re-tested in devices as shown in panel G and H. Sample 17 was also tested twice (panel F and H) as in the first run (panel F), one of the duplicates showed amplification. This observation was consistent on repeating the test for sample 17 in panel H, where again only one of the duplicates showed amplification. All four of the sample 17 test results were also analyzed using gel electrophoresis to confirm the results from FLIPP-NAAT. The results were found to be consistent and are explained in the next section. Only one anomaly was found during testing of these 30 clinical samples, where sample 9 showed a positive test result in panel (C) but not in panel (H). Though device in panel (C) was deemed as a failed test, both the positive and negative controls in the module for sample 9 had worked perfectly fine. The ambiguity was resolved by analyzing the amplicons for sample 9 from device H using gel electrophoresis and the details are explained in the next section.

Supplementary Figure S7. New protocol of TB testing for smear negative clinical samples in FLIPP-NAAT

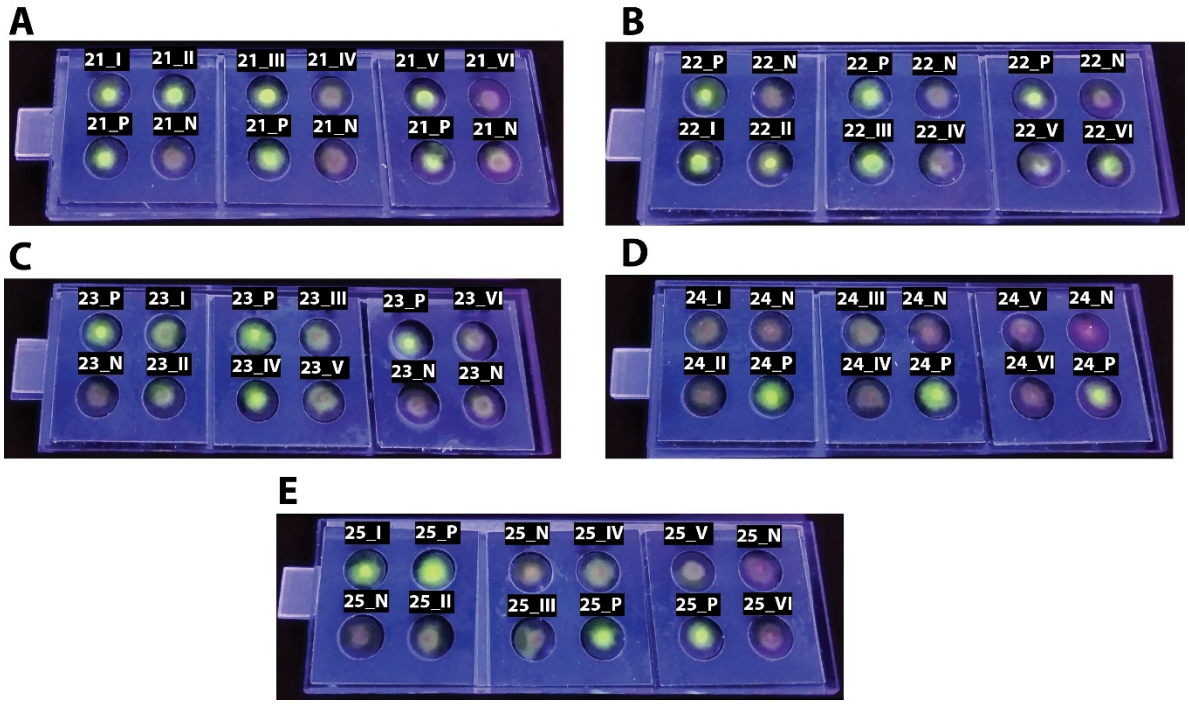

Supplementary Figure S7. TB testing in FLIPP-NAAT for lower bacillary load clinical samples. The five sputum smear microscopy negative clinical samples were tested in FLIPP-NAAT with six replicates per sample instead of duplicates and the results were captured using a cell phone camera. Numbers on top of each testing zone represent the sample number. Each sample was tested in duplicates and suffix 'I, II, III, IV, V and VI' represent the duplicates for each sample. N – Negative control. P – Positive control.

A loss in amplification was observed for sputum smear negative samples when the results for testing in FLIPP_NAAT (for duplicates per sample) were compared with the results from GeneXpert. This was attributed to the very small amount of starting template added to the reaction zones and the challenge was solved by running a greater number of replicates per sample. Six replicates were run per sample for the 5 sputum smear negative GeneXpert positive samples and the test was deemed to be positive if at least one out of the six replicates showed amplification.

Supplementary Figure S8. Gel electrophoresis results for TB testing from clinical samples

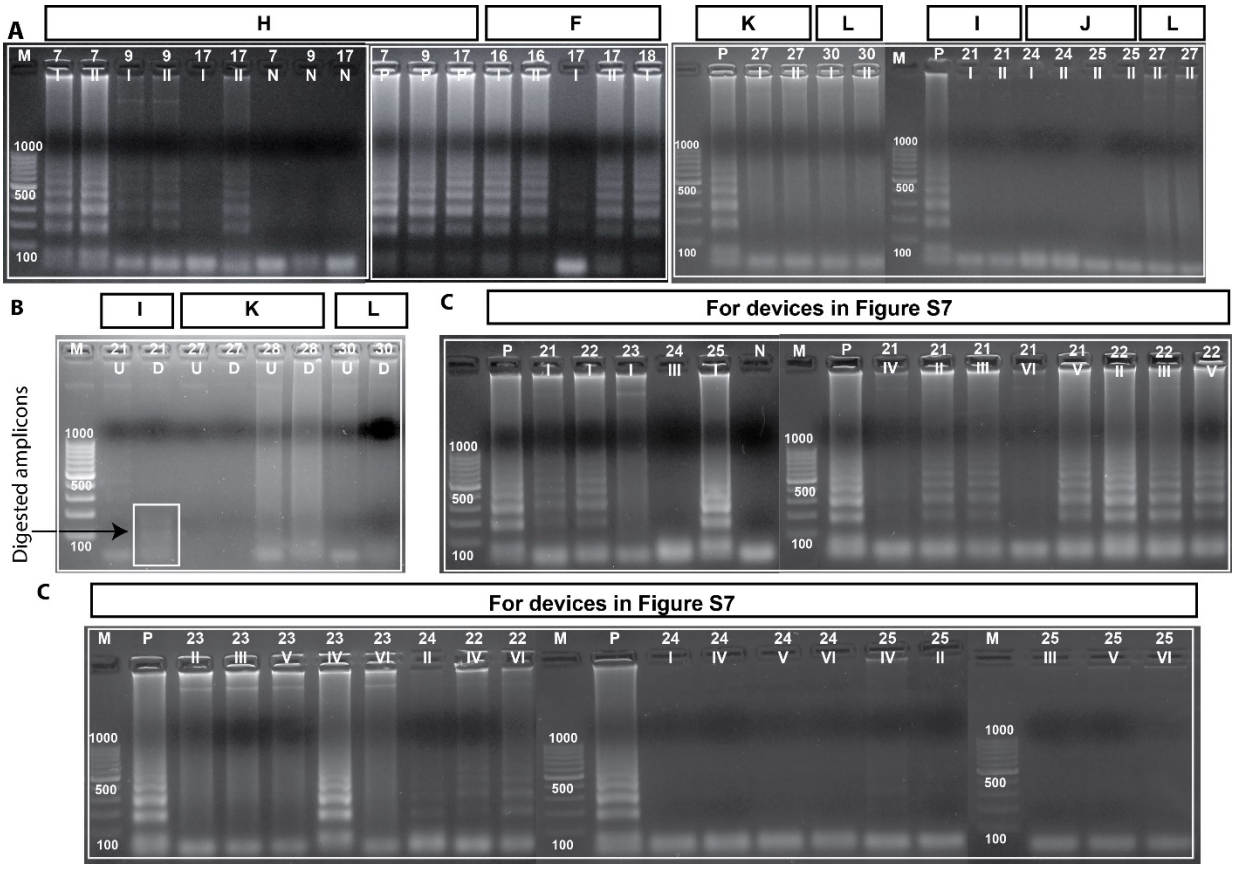

Supplementary Figure S8. Confirmation of LAMP patterns for amplification from clinical samples in FLIPP-NAAT. DNA amplification was performed in FLIPP-NAAT, amplicons were eluted from paper as explained in Fig. 5 in the main manuscript and the products were analysed using gel electrophoresis. The numbers on top of each well represent the sample number and suffix 'I, II, III, IV, V and VI' represent sample duplicates. M – DNA ladder, N – negative control, P – positive control, U- Undigested amplicons and D- digested amplicons. (A) Comparison of gel patterns for amplification from clinical samples to confirm the banding patterns. (B) Digestion of amplicons from clinical sample to confirm target-specific amplification. (C) Comparison of gel patterns for amplification from smear negative clinical samples to confirm the banding patterns. Alphabets on the top of gel lanes correspond to figure panels in Supplementary figure S6. The lanes marked within a white box are from the same gel and original gel images have been used.

LAMP amplicons from the reaction zones of the device from panel H, F, K, L, I, J and devices in Supplementary figure S8 were analyzed using gel electrophoresis. The gel patterns obtained for all the true positive clinical samples were identical to the positive controls which were set-up using 3.5 µl of 100copies/ µl of purified *Mtb* gNDA. However, the gel patterns for the false positive samples (Sample 27,28 and 30) we completely different from the target-specific

amplification pattern and the amplicons also did not get digested using the restriction enzyme *AatII*. All the negative controls did not show any amplification. Consistent with the FLIPP-NAAT results, sample 17_I in device H did not show any amplified products on the gel, while sample 17_I from device F showed very faint bands. This was also corroborated by the smear microscopy and GeneXpert results, both of which had classified sample 17 as weakly infected. Since one of the duplicates for sample 17 showed consistent amplification, sample 17 was considered as positive for FLIPP-NAAT test results.

Even though sample 9_I and 9_II from the device in panel H appear slightly green to the eye, the intensity from the test zones was not found to be higher than the threshold during the intensity analysis (Supplementary table S4). The gel results for sample 9_I and 9_II from device in panel H helped in resolving the ambiguity and confirming that sample 9 is a true positive.

Supplementary Figure S9. Uncropped images for gel electrophoresis analysis

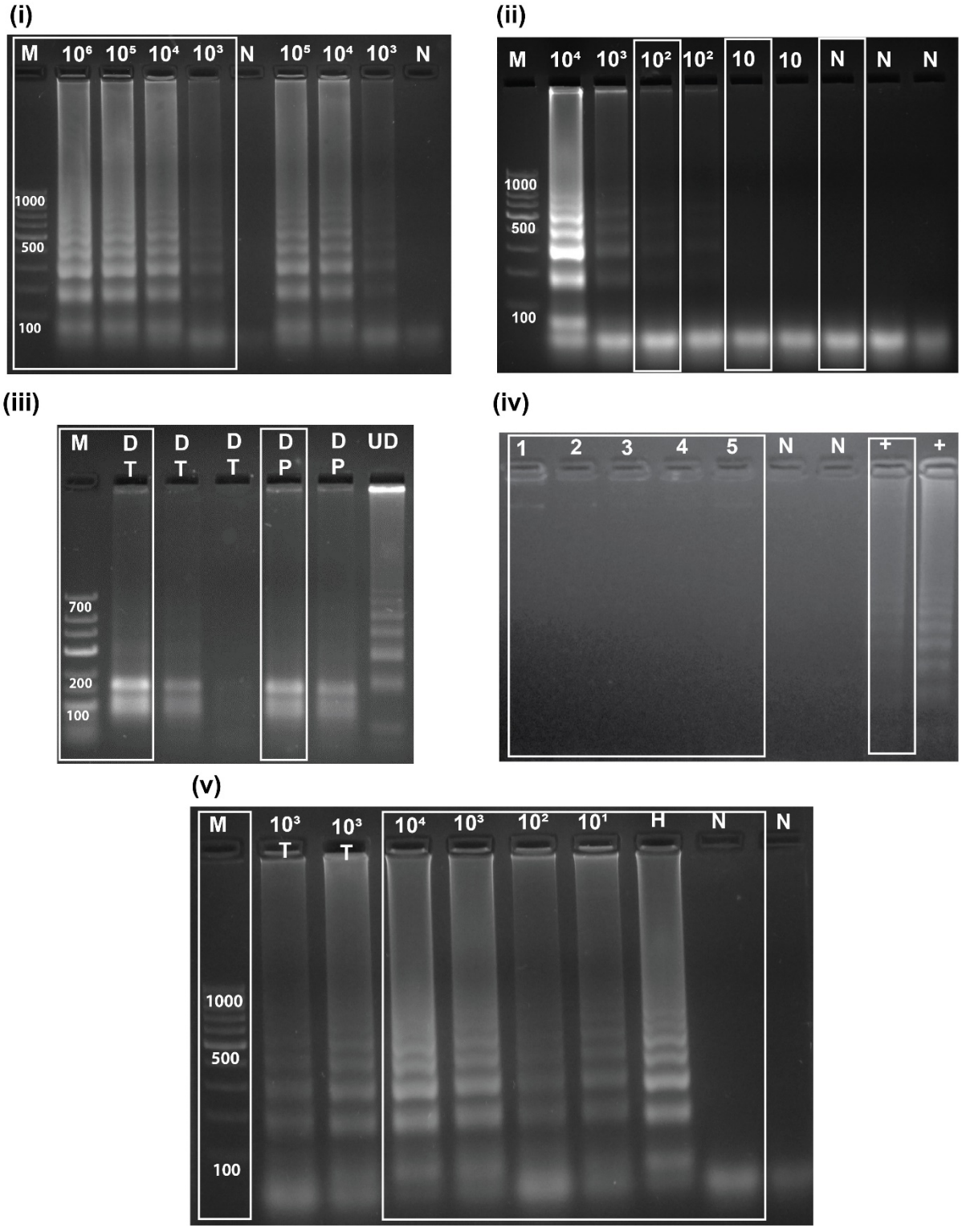

Supplementary Figure S9. Uncropped images for gel electrophoresis analysis. Sections marked within white boxes represent the lanes used in the figures for the main manuscript. **(i), (ii)** and **(iii)** LAMP in tube. Gel electrophoresis analysis of products of LAMP reactions conducted in tube with varying starting

copy numbers of Mtb gDNA (10^6copies up to 10 copies). The numbers on top of the lanes indicate the starting copy number of the template. N- No template control, M- DNA marker and D- digested LAMP amplicons. Reaction time was 40 minutes. **(iv)** Specificity of the LAMP assay tested against non-Mtb targets. +: Positive control (Mtb gDNA), 1: plasmid with hepatitis C insert, 2: plasmid with dengue insert, 3: E. coli gDNA, 4: Human gDNA, 5: Mycobacterium smegmatis gDNA. LAMP amplification in paper. **(v)** Gel electrophoresis analysis of products of LAMP reactions conducted in paper starting from varying number of starting Mtb gDNA copies (10^4 up to 10). The numbers on top of the wells indicate the starting copy number of the template. H- 1000 copies of human gDNA were added to the reaction mix along with 1000 copies of Mtb gDNA; N- No template control; M- DNA marker; and D- digested LAMP amplicons. T- LAMP reaction in tube and P- LAMP reaction in paper. The reaction time was 40 minutes.

Supplementary Methods

Extraction of DNA from Mtb cultures

DNA obtained from Mtb bacterial cultures (strain H37Ra) was extracted using two methods: i) QIAamp DNA mini kit (Qiagen, 51304), and ii) an in-house crude boiling method. In the former, Mtb cells were lysed and DNA extracted following the protocol recommended by the manufacturer; 1 µl of the solution collected at the end of the extraction protocol was directly added to the LAMP mix. In the latter (in-house) method, 1ml of Mtb bacterial cell culture was centrifuged at 7000 rpm for 5 minutes to pellet down the bacterial cells. The supernatant was removed, and the pellet was resuspended in 200 µl TE buffer (10mM Tris base, 1mM EDTA). The resulting suspension was vortexed and kept at 95˚C for 30 minutes to lyse the cells. The turbid solution obtained was centrifuged at 8000 rpm for 5 minutes and 1 µl of the supernatant was directly added to the LAMP mix.

Supplementary Notes

Supplementary Note S1. Why LAMP?

While several isothermal nucleic acid amplification techniques exist, we chose LAMP for FLIPP-NAAT because of its multiple distinctive characteristics, e.g. i) enhanced specificity because of

the need of at least 4 primers, ii) an operating temperature range of 60-65˚C that is far from ambient, reducing baseline enzyme activity during storage, and iii) it's non-proprietary nature that enables acquiring individual reaction components from different vendors, providing flexibility for cost reduction. There are, however, certain challenges associated with LAMP. Primer dimer formation in LAMP leads to ladder-like patterns on gels reminiscent of target-specific amplification. Target-specific and non-specific amplification can be distinguished only by conducting enzyme digestion of products. The larger challenge with LAMP, however, is that because the number of amplicons produced is high, the method is prone to carryover amplicon contamination via aerosols. Post-amplification analysis was always conducted in a separate laboratory from the one in which LAMP reactions were set-up to avoid carryover contamination.

Supplementary Note S2. Comparison of FLIPP-NAAAT with existing similar designs

The device design by Seok et al.[1] and Ahn et al.[2] consisted of an assembly of polysulphone membrane, wax patterned polyethersulphone membrane, and glass fiber; physically stacked one above another and covered with ELISA sealing tape. The assembly was placed in a petri dish containing moist toilet tissues to maintain humidity and the petri dish was sealed using an aluminum tape. Nucleic acid amplification was demonstrated using LAMP and recombinase polymerase amplification (RPA). Fluorescence measurements were recorded at 10-min intervals by taking the set-up out of the oven and it was placed back at 63 °C in the oven immediately after measurement. The device from Trinh and Lee[3] consisted of a CNC milled pattern on a middle polycarbonate layer sandwiched between two sealing films. The chip was centrifuged after sample addition to distribute the sample to the respective reaction zones. Both the studies used fluorescence-based detection with imaging done in a high-end Bio-Rad Molecular Imager Gel ChemiDoc. Both the designs had multiple user steps, required ancillary equipment, and

fluorescence imaging was done in an expensive set-up. FLIPP-NAAT, on the other hand, can contain all the components required for NAATs within the device and the user experience is very simple and minimal. One of the most desirable features of FLIPP NAAT is that the material cost of making a 12-reaction-zone device is only $0.88 and the cost of reagents required per reaction zone is $0.43 (see Supplementary Table S3 and S4 online). Modular design is a powerful feature of FLIPP-NAAT and using the current definition of a module, devices may be designed to contain 4N reaction zones (where N = 1, 2, 3…), without any major modification in fabrication methods. The device design is a simple layer-by-layer assembly of paper pads, plastics, and adhesives, and therefore it is compatible with mass manufacturing using injection molded plastic components. The very low-cost imaging box designed for cell phone-based filter-free fluorescence imaging is also an important development for enabling point-of-care NAATs.

Supplementary Note S3. Optimizing FLIPP-NAAT design

Several design challenges were overcome to develop the final FLIPP-NAAT prototype. Because the paper reaction zones in FLIPP-NAAT are in close proximity to each other, cross contamination was a challenge. The device dimensions were modified to provide more area of contact for the PSA to ensure it did not detach during heating at 63˚C. A vice was used to pressurize the device after fabrication to ensure that all layers were tightly secured. In the current design, there exists a 1-mm gap between modules, where there is discontinuity in both the top black acrylic covers and the bottom layer of PSA. The sudden change in surface properties from PSA to acrylic in these gaps helps in avoiding spread of leaking fluid, if any. Different types of materials were iterated to determine the most suitable material for each layer to optimize fluorescence detection. Transparent acrylic bottom allowed imaging from the bottom. Black acrylic covers, PSA, and the transparency cover gave minimum background fluorescence. The entirely plastic assembly of the device (i.e. no

use of glass) made it amenable to pressurized sealing, which created evaporation-free reaction zones and avoided cross-talk between the reaction zones.

References:

1. Seok, Y. *et al.* A Paper-Based Device for Performing Loop-Mediated Isothermal Amplification with Real-Time Simultaneous Detection of Multiple DNA Targets. *Theranostics* **7**, 2220–2230 (2017).
2. Ahn, H., Batule, B. S., Seok, Y. & Kim, M. G. Single-Step Recombinase Polymerase Amplification Assay Based on a Paper Chip for Simultaneous Detection of Multiple Foodborne Pathogens. *Anal. Chem.* **90**, 10211–10216 (2018).
3. Trinh, T. N. D. & Lee, N. Y. A rapid and eco-friendly isothermal amplification microdevice for multiplex detection of foodborne pathogens. *Lab Chip* **18**, 2369–2377 (2018).